JOURNAL OF SOLID STATE CHEMISTRY 75, 90–98 (1988)

# Crystallographic and Magnetic Structure of $Li_2MnO_3$

PIERRE STROBEL AND BERNADETTE LAMBERT-ANDRON

*Laboratoire de Cristallographie CNRS, associé à l'U.S.T.M.G., 166X, 38042 Grenoble Cedex, France*

Received November 4, 1987, in revised form January 11, 1988

The structure of $Li_2MnO_3$ was refined on a single crystal: space group $C2/m$, $a = 493.7(1)$, $b = 853.2(1)$, $c = 503.0(2)$ pm, $\beta = 109.46(3)°$, $Z = 4$, $R = 0.020$, $R_w = 0.027$ for 619 independent reflections with $I > 5\sigma$. Distortions in the ordered rocksalt superstructure are induced by the *cis* positions of $Mn^{4+}$ in the $O^{2-}$ coordination octahedra. Powders of $Li_2MnO_3$ are slightly disordered with $12 \pm 3\%$ Mn on the Li sites. They are antiferromagnetic with $T_N = 36.5$ K; the cell is doubled along $c$, corresponding to opposite moments on alternating Mn-containing layers along $c$. A comparison of structural data of rocksalt-related $A_2BO_3$ compounds ($A$ = Li, Na; $B$ = tetravalent metal) shows that many previously reported cells could be indexed in smaller monoclinic or hexagonal cells. 

## Introduction

During a study of hydrothermal syntheses in the Li–Mn–O system, single crystals of $Li_2Mn^{IV}O_3$ were grown (*1*). This compound is known to crystallize in the $Li_2SnO_3$-type structure, an ordered rocksalt superstructure with cationic (111) planes alternatively occupied by Li and by ($LiSn_2$) layers (*2*). There is some confusion in the literature about the actual cell symmetry of $Li_2MnO_3$ (given as orthorhombic (*2*) or monoclinic $C2/c$ (*3*), but cubic and hexagonal forms were also reported (*4*)). No single-crystal structure refinement has been published. In the $Li_2SnO_3$ structure, tetravalent cations lie in layers (forming a honeycomb planar sublattice for complete ($LiM_2^{4+}$) ordering) separated by O, Li, and O layers. $Li_2MnO_3$ orders antiferromagnetically at ≈50 K (*3*), as expected for octahedral site $d^3$ ions with edge-sharing between adjacent octahedra (*5*). The $Mn^{4+}$ sublattice, however, differs from that in other $Mn^{4+}$-containing antiferromagnetic oxides for which the magnetic structure has been determined, like $\beta$-$MnO_2$ (rutile-type) and $BaMnO_3$, which contain infinite linear chains of edge- or face-sharing ($Mn^{4+}O_6$) octahedra (*6, 7*), and $Ca_2MnO_4$, with $K_2NiF_4$ type structure (*8*).

We present in this paper (i) a single-crystal refinement of the $Li_2MnO_3$ structure and (ii) the determination of its magnetic structure below $T_N$ by powder neutron diffraction. It will be shown that single crystals belong to a cell symmetry different from all those previously proposed, and that Li–Mn disorder occurs in powders prepared by solid-state reaction. The magnetic structure involves a doubling of the crystallographic cell in the direction perpendicular to the cation layers. Finally, the relationships between the various cells proposed in the rocksalt-related $A_2BO_3$ compounds are discussed.

0022-4596/88 $3.00

## Experimental

The synthesis of single crystals of $Li_2MnO_3$ has been described previously (*1*). The crystal used in this study was obtained from a lithium chloride flux. Powder samples for neutron diffraction were prepared by repeated firings of stoichiometric mixtures of lithium carbonate and $\beta$-manganese dioxide at 850°C, with intermittent grindings. A final annealing at 1000°C for 50 hr resulted in a significant narrowing of the X-ray diffraction lines of the powdered sample. Preliminary examination using precession photographs were consistent with Jansen's proposed space group $P2/c$ (*3*).

A single crystal of $Li_2MnO_3$ with dimensions $0.16 \times 0.14 \times 0.04$ mm$^3$ was examined using a computer-controlled Enraf–Nonius CAD4 X-ray diffractometer at 293 K. Ag$K\alpha$ radiation was used with the $\omega$-scan mode in the range $2 < \theta < 30°$ with 1.5° scan range. The standard reflections were monitored after every 200 reflections. A total of 2465 reflections were collected over a half-sphere, yielding 619 independent data by averaging equivalent reflections with $I > 5\sigma$. No absorption correction was performed. The lattice parameters were obtained by least-squares refinement of the setting angles of 25 reflections with $2\theta > 20°$, using $\lambda$(Ag$K\alpha$) = 0.55936 Å.

Powder neutron diffraction spectra were recorded between 4 and 80 K using the D1B high-resolution powder diffractometer at the Institut Laue-Langevin, Grenoble. A neutron wavelength of 2.522 Å was used to collect data at $2\theta$ intervals of 0.2° in the angular range $10 < 2\theta < 90°$. The sample (ca. 15 g) was placed in a cylindrical vanadium container of 12 mm diameter.

## Results and Discussion

### *1. X-Ray Structure Determination*

*Space group and cell parameters.* Examination of the data revealed that all reflections indexed in Jansen's cell obeyed the condition $h + k + l$ all odd or all even (this condition is also met in Jansen's powder diagram (*3*)). This $F$-cell was converted into a monoclinic $C$-cell with halved cell volume using the following transformation matrix (J= Jansen's, S = Strobel's cell):

$$\begin{bmatrix} a_S \\ b_S \\ c_S \end{bmatrix} = \begin{bmatrix} -1 & 0 & 0 \\ 0 & -1 & 0 \\ \frac{1}{2} & 0 & \frac{1}{2} \end{bmatrix} \begin{bmatrix} a_J \\ b_J \\ c_J \end{bmatrix}. \quad [A]$$

Refined cell parameters at 293 K are $a$ = 493.7(1), $b$ = 853.2(1), $c$ = 503.0(2) pm, $\beta$ = 109.46(3)°, $Z$ = 4. Possible space groups were $C2$ or $C2/m$. A piezoelectricity test on $Li_2MnO_3$ powder was negative. Wilson's symmetry test also supported the centrosymmetrical group, and we considered the space group to be $C2/m$.

*Structure refinement.* The manganese atomic positions were determined using the Patterson method. Oxygen and lithium atomic positions were subsequently revealed by Fourier and difference-Fourier maps. All atomic positions were refined with an isotropic full-matrix least squares using the SDP package on a PDP-11 computer. Anisotropic thermal parameters of Li1, a very light atom in a special position, could not be refined. The final residuals were $R$ = 0.020 and $R_w$ = 0.027, where $R_w = [\Sigma w(|F_o| - |F_c|)^2/\Sigma w F_o^2]^{1/2}$ with $w = 1/\sigma(F_o)^2$ (a list of observed and calculated structure factors is available on request). The final positional parameters are listed in Table I. Bond distances are listed in Table II.

*Structure description.* The structure is essentially as proposed from powder work by Jansen and Hoppe (*3*). These authors, however, did not notice the occurrence of a mirror plane parallel to the $ac$ plane in their cell. This mirror results from the stacking of the ($Mn_2Li$) layers, which differs from that in $Li_2SnO_3$ (see Fig. 1). They noted that the structure is pseudo-orthorhombic with

TABLE I

FINAL POSITION AND THERMAL PARAMETERS[a] OF $Li_2MnO_3$ AT 293 K

| Atom | Site | $x$ | $y$ | $z$ | $\beta_{eq}$ | $\beta_{11}$ | $\beta_{22}$ | $\beta_{33}$ | $\beta_{12}$ | $\beta_{13}$ | $\beta_{23}$ |
|---|---|---|---|---|---|---|---|---|---|---|---|
| Mn | 4g | 0 | 0.16708(2) | 0 | 0.244(2) | 0.00251(4) | 0.00063(2) | 0.00365(4) | 0 | 0.00199(7) | 0 |
| Li1 | 2b | 0 | 0.5 | 0 | 0.28(3)[b] | | | | | | |
| Li2 | 2c | 0 | 0 | 0.5 | 1.10(6) | 0.013(1) | 0.0047(4) | 0.0103(10) | 0 | 0.013(2) | 0 |
| Li3 | 4h | 0 | 0.6606(3) | 0.5 | 1.01(4) | 0.012(1) | 0.0030(3) | 0.0101(9) | 0 | 0.002(1) | 0 |
| O1 | 4i | 0.2189(2) | 0 | 0.2273(2) | 0.41(1) | 0.0046(2) | 0.00104(7) | 0.0053(2) | 0 | 0.0016(3) | 0 |
| O2 | 8j | 0.2540(1) | 0.32119(7) | 0.2233(1) | 0.420(7) | 0.0048(2) | 0.00142(5) | 0.0050(2) | −0.0009(1) | 0.0039(3) | −0.0007(1) |

[a] Anisotropic thermal parameters are defined by $T = \exp[-(\beta_{11}h^2 + \beta_{22}k^2 + \beta_{33}l^2 + \beta_{12}hk + \beta_{13}hl + \beta_{23}kl)]$.
[b] Not refined anisotropically.

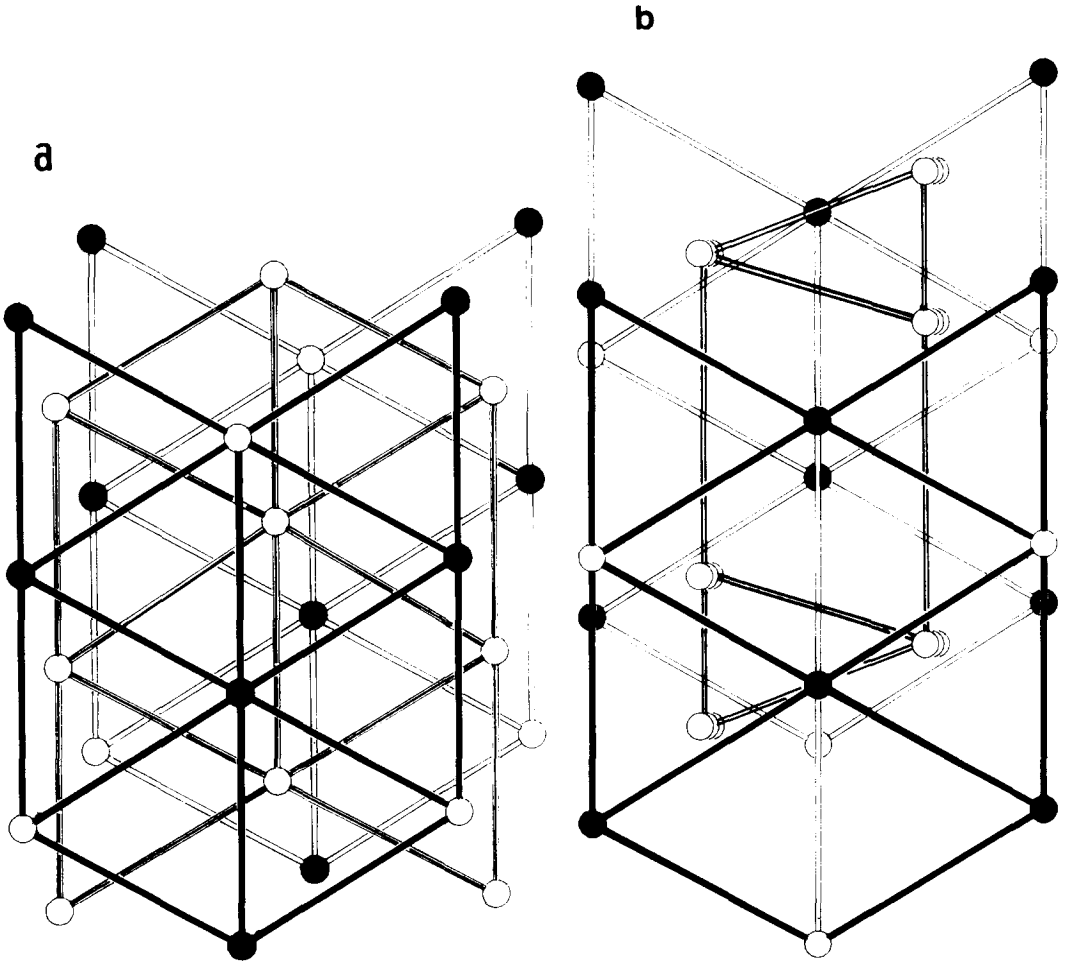


FIG. 1. ORTEP *ab* plane projections of the structures of $Li_2MnO_3$ (a) and $Li_2SnO_3$ (b, from Ref. (*19*)), showing three successive layers along *c*. Filled circles, Mn or Sn; open circles, Li; anions (in cubic compact arrangement) are omitted for clarity.

TABLE II

INTERATOMIC DISTANCES IN Li2MnO3 AT 293 K (IN pm)

| | |
|---|---|
| Mn–O1 | 191.90(5) [×2] |
| Mn–O2 | 190.38(6) [×4] |
| Li1–O1 | 206.98(11) [×2] |
| –O2 | 205.39(6) [×4] |
| Li2–O1 | 200.87(11) [×2] |
| –O2 | 214.68(6) [×4] |
| Li3–O1 | 210.12(19) [×2] |
| –O2 | 216.60(8) [×4] |
| Mn–Mn(1) | 285.01(3) |
| –Mn(2) | 284.41(1) |

*Note.* Estimated standard errors in parentheses.

$l_o = (h_J + 3l_J)/2$. But this relationship implies $h_J + l_J = 2n$. In conjunction with the *C*-centered lattice condition $h_J = k_J = 2n$, this results in ($h_J$, $k_J$, $l_J$) all odd or all even, i.e., a face-centered lattice, therefore, the cell transformation to a *C*-cell of half volume used here ($Z = 4$). Bond distances and angles (Table II) show that the ($Mn_2Li1$) layers are little distorted. The six Mn–O distances are equal within 0.8%, and the same applies to Li1–O distances. $Mn^{4+}$ ions (ionic radius 53 pm (*9*)) fit octahedral sites of the close-compact oxide network quite well (theoretical octahedral site radius: $140(\sqrt{2} - 1) = 58$ pm). Li–O bond lengths for Li1 (average 205.9 pm) and in the Li-only layer (average 210.2 pm for both Li2 and Li3) are significantly shorter than the sum of ionic radii (216 pm). All coordination octahedra are distorted. Two effects contribute to the distortions: (i) the size difference between $Mn^{4+}$ and $Li^+$, (ii) the high charge on $Mn^{4+}$ ions, which occur in *cis* position in the coordination octahedra of oxide ions. The Mn–Mn repulsion is minimized by large Mn–O–Mn angles (see Fig. 2a). This in turn gives cation coordination polyhedra with small O–*M*–O angles for the O–O edges shared with neighboring $MnO_6$ octahedra (81.6 to 84.4°) (see Fig. 1b). Bond distances are more scattered in the Li-only layers than in the ($Mn_2Li1$) layers. The $Li2O_6$ octahedron is compressed along the *trans* O1–O1 direction, while the $Li3O_6$ octahedron includes three different Li–O distances (see Fig. 2). The $\beta$ angle corresponds within experimental errors to the dihedral angle between faces of the regular octahedron (109.47°).

### 2. *Magnetic Structure at 4.2 K*

Neutron diffraction patterns on annealed powder below $T_N$ exhibit magnetic reflections, which can be indexed with a propagation vector $\mathbf{k} = [00\frac{1}{2}]$, i.e., in a cell with doubled *c* parameter (see Fig. 3). The cell constants at 4.2 K are $a = 492.9(6)$, $b = 850.3(8)$, $c = 1004.0(12)$ pm, $\beta = 109.29(8)°$. These features confirm the occurrence of antiferromagnetism with moments of opposite signs at *z* and $z + 1$. The value of $T_N$, extrapolated from the temperature variation of magnetic reflection intensities (Fig. 4) is $36.5 \pm 0.5$ K. All magnetic reflections obey the condition $h + k = 2n$. The magnetic ions $Mn^{4+}$ (labeled 1 . . . 4) occupy the position 4(g) in the crystal cell, namely:

(1) 0, *y*, 0; (2) $\frac{1}{2}$, $y + \frac{1}{2}$, 0;
(3) 0, $-y$, 0; (4) $\frac{1}{2}$, $\frac{1}{2} - y$, 0.

Using Bertaut's macroscopic method (*10*), which supposes that the Heisenberg–Néel exchange hamiltonian remains invariant for the propagation vector **k** in the $C2/m$ group operations, the possible spin configurations are,

$$\Gamma_{1g}: F_y = S_{1y} + S_{2y} + S_{3y} + S_{4y}$$

$$\Gamma_{2u}: C_x = S_{1x} + S_{2x} - S_{3x} - S_{4x};$$
$$C_z = S_{1z} + S_{2z} - S_{3z} - S_{4z}$$

$$\Gamma_{3g}: F_x = S_{1x} + S_{2x} + S_{3x} + S_{4x};$$
$$F_z = S_{1z} + S_{2z} + S_{3z} + S_{4z}$$

$$\Gamma_{4u}: C_y = S_{1y} + S_{2y} - S_{3y} - S_{4y},$$

where the $\Gamma$'s are the irreducible representations of the group.

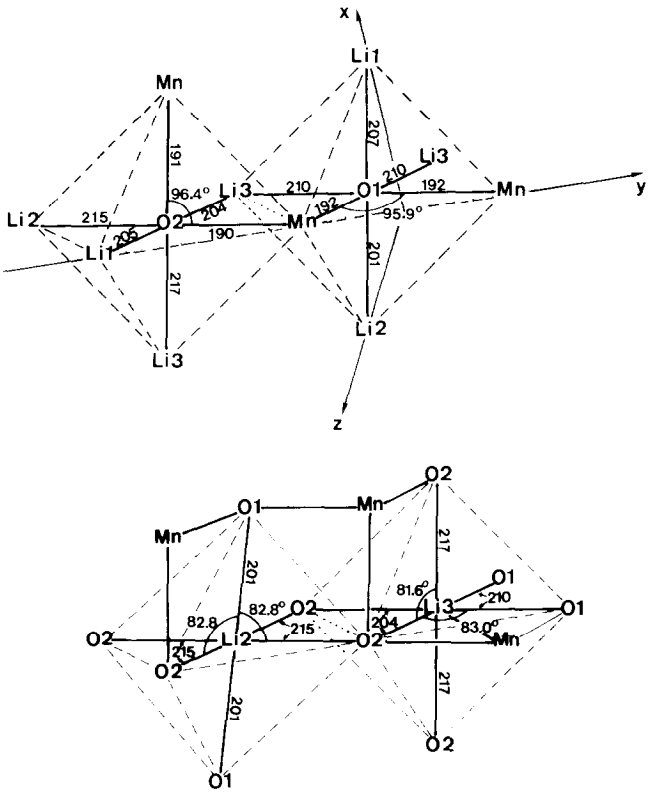


FIG. 2. Coordination octahedra (with interatomic distances in pm) and angles of O (top) and Li in the Li layers (bottom).

For a collinear structure, the magnetic intensity is given by

$$I_n = \frac{e^2\gamma^2}{mc^2} \cdot F_M^2(\mathbf{h}) \sin^2\alpha,$$

where $e$, $m$, and $c$ have their usual meaning, $\gamma$ is the neutron magnetic moment, $F_M$ is the magnetic structure factor, and $\alpha$ is the angle between the spin direction and the diffusion vector $\mathbf{h}$. From the absence of 001 reflections, only the $F_z$ component is permitted for the $F$ mode.

Difficulties in obtaining reasonable values of the Mn atom magnetic moment prompted us to refine the X-ray pattern of the powder used for neutron diffraction work. This X-ray line intensity fitting (*11*) showed evidence of manganese vacancies on the 4g site. The reliability factors, $R_w$, are 0.11 and 0.07 for a 4g site occupation by Mn atoms equal to 1 and 0.88 ± 0.03, respectively. The latter solution corresponds to a $Mn_{(4g)}$ vacancy fraction equal to ≈0.12. The number of observed intensities is not sufficient to determine accurately a possible distribution of Mn atoms on Li sites. This effect could not be seen so clearly from the neutron spectra, because of the fairly small difference between the Fermi lengths of Li and Mn (−0.35 and −0.22 $10^{12}$ cm, respectively (*13*)). Partial exchange of 0.12 Mn for Li on octahedral sites is quite possible in such a structure, in view of the similarity in ionic radii between $Li^+$ and

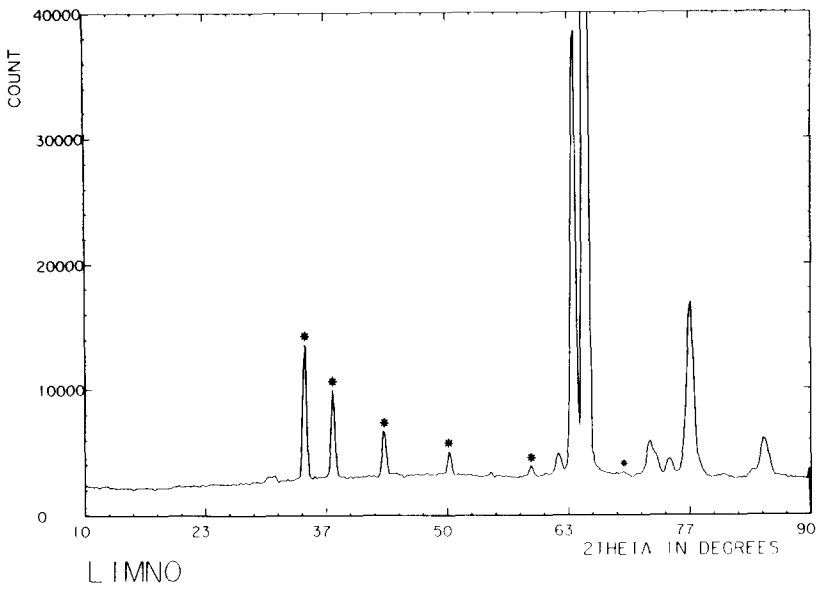


FIG. 3. Powder neutron diffraction pattern at 4.2 K; * = magnetic reflections (for their indexation, see Table III).

$Mn^{4+}$ and common occurrence of cationic disorder in $A_2BO_3$ structures (see Section 3).

Taking into account this manganese atomic disorder, least-squares refinements of the possible models (*12*) gives the best agreement between calculated and observed intensities for the solution $F_z = S_{1z} + S_{2z} + S_{3z} + S_{4z}$ with $R = 0.045$ (Table III). Magnetic form factors were taken from Ref. (*14*). The scale factor was determined from the ratio of observed and calculated nuclear intensities. The experimental magnetic moment $\mu_{Mn}$ is (2.7 ± 0.3) Bohr magnetons, in good agreement with the spin-

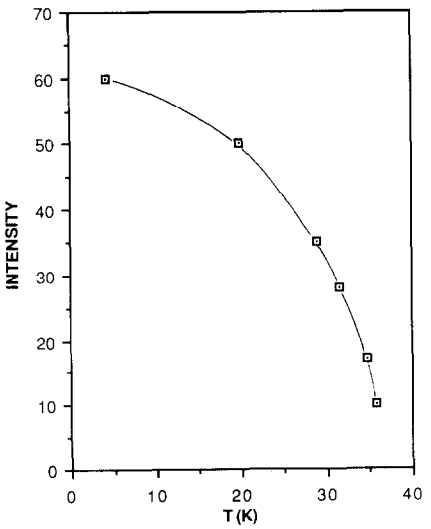


FIG. 4. Intensity of the magnetic (−111) reflection as a function of temperature.

TABLE III

OBSERVED AND CALCULATED MAGNETIC INTENSITIES AT 4.2 K

| $h$ | $k$ | $l^a$ | $I_{obs.}$ | $I_{calc}$ |
|---|---|---|---|---|
| −1 | 1 | 1 | 3.99(12) | 3.692 |
| 0 | 2 | 1 | 3.03(8) | 3.104 |
| 1 | 1 | 1 | 2.15(10) | 2.158 |
| −1 | 1 | 3 | 1.30(8) | 1.447 |
| 0 | 2 | 3 | 0.79(12) | 0.940 |
| 2 | 2 | 1 | 1.20(25) | 0.973 |

[a] Indexed in magnetic (*c*-doubled) cell.

only theoretical magnetic moment of $Mn^{4+}$. The $C_z$ solution also yields a satisfactory fit ($R = 0.050$), but with an unrealistically small value of $\mu_{Mn}$ ($<\approx 1\ \mu_B$).

The solution $F_z$ corresponds to a ferromagnetic arrangement of the spins in the ($Mn_2Li$) planes, with antiparallel stacking of these layers along **c**. It can be compared to that of $Ca_2MnO_4$, another oxide with a layered arrangement of the $Mn^{4+}$ sublattice ($K_2NiF_4$ structure) (*8*). Both give rise to an antiparallel stacking of the layers along **c**. In the layers, however, the interactions are found to be of opposite sign. One significant difference in the superexchange paths between the $K_2NiF_4$ and $Li_2MnO_3$ structures should be pointed out. The $MnO_6$ octahedra share corners in the former and edges in the latter, leading to Mn–O–Mn angles equal to 180 and ≈90°, respectively. For $d^3$ ions, the 90° superexchange angle gives rise to both positive and negative interactions (*5*). Given the additional difficulty introduced by the manganese vacancies, a comprehensive discussion of these interactions has not been attempted.

### *3. On the Crystal Chemistry of $A_2BO_3$ Compounds*

Numerous $A_2BO_3$ compounds have been reported in Jansen's cell ($Z = 8$), which is typified by $Li_2SnO_3$, or in an orthorhombic *C*-centered cell to which it can be reduced when $\cos\beta_J = -a_J/3c_J$ ($\mathbf{c}_0 = -\mathbf{a}_J - 3\mathbf{c}_J$) (*2*). These cells will be referred to hereafter as mC8 and oC24 cells, respectively (where m and o stand for "monoclinic" and "orthorhombic," and the numerals are equal to *Z*). The crystal chemistry of $A_2BO_3$ compounds derived from the rocksalt structure type is actually more complex. Polymorphism has been reported in numerous compounds (see Table 2 in Ref. (*15*)). Depending on cation ordering and site distortions, the symmetry can vary from cubic to monoclinic. Single-crystal data were available previously for two compounds only, and the published structural refinement yielded rather high *R* values for both (see Table IV). A survey of compounds reported as "$Li_2SnO_3$ type" (with powder X-ray patterns indexed in the mC8, oC24, or oC12 cell) shows that, within the accuracy of the data, most of these patterns obey (i) the face-centered condition ($h, k, l$) all odd or all even, (ii) the metric condition for orthorhombic symmetry $\cos\beta_J = -a_J/3c_J$, (iii) the metric condition for hexagonal symmetry $b/a = \sqrt{3}$ (see Table IV).

Lang (*2*) studied the symmetries resulting from various stackings of the $AB_2$ layers along *c*. The "most probable" stackings correspond to space groups $C2/m$ ($Z = 4$), $P3_212$ ($Z = 6$), and $C/c$ ($Z = 8$). Structural refinements confirm this: for $A_2BO_3$ compounds synthesized in single-crystal form (i.e., annealed for long periods in thermodynamic equilibrium conditions), structural studies lead to mC cells with $Z = 4$ ($Li_2ZrO_3$, $Li_2MnO_3$) or $Z = 8$ ($Li_2TiO_3$, $Li_2SnO_3$), with the expected space group. In the case of $Li_2ZrO_3$, a recent neutron powder diffraction study (*16*) gave a $C2/c$ ($Z = 4$) cell corresponding to a cation distribution different from the $Li_2SnO_3$ type ([$Li_2Zr$] layers only). The symmetry of powders obviously depend on their preparation conditions, as shown by several examples of polymorphism. For $Li_2MnO_3$, we noticed that powders annealed at 1000°C showed X-ray and neutron diffraction lines much sharper than those synthesized at ≈850°C, but the indexation is identical and consistent with the single-crystal cell mC4 (for monoclinic *C*-centered with $Z = 4$) [Cubic and hexagonal polymorphs were prepared by slow decomposition of $Li_3MnO_4$ at low temperature (*4*)]. Moreover, Hodeau *et al.* (*16*) showed that $Li_2SnO_3$ powder contains lithium vacancies. Most literature data for powders prepared by solid-state reaction, which were indexed using the mC8 (or mC24 with tripled *c* parameter), oC12, oC24 cells (and in the case of $Na_2SnO_3$, in a

TABLE IV

CRYSTAL DATA FOR ROCKSALT-RELATED $A_2BO_3$ COMPOUNDS

| Compound | Reference[a] | Published cell[b] | Notes[c] | Alternate indexation (parameters in pm) |
|---|---|---|---|---|
| $Li_2TiO_3$ | (*17*) | mC8 | XCR $C2/c$ | |
| | 8-249 | | $R$ = 8.6% for $n$ = 460 | |
| $Li_2ZrO_3$ | (*16*) | mC4 | NPR $C2/c$, $R$ = 5.01% | |
| | | | all [$Li_2Zr$] layers similar | |
| $Li_2HfO_3$ | 23-1183 | mC4 | | |
| $Li_2MoO_3$ | $\alpha$: 21-517 | cF32/3 | | |
| | $\beta$: 21-515 | mC8 | $hkl$ all even | h6: $a$ = 496.6(2) |
| | (*18*) | | $\Delta\beta < 0.1°$ | $c$ = 1493(1) |
| | | | $b/a$ = 1.732 | |
| $Li_2MnO_3$ | (*4*) | cF4/3 | Low-temp. form | |
| | | h6 | Low-temp. form | |
| | This work | | XCR $C2/m$ | mC4 |
| | | | $R$ = 2.0% for $n$ = 619 | |
| $Li_2PdO_3$ | 30-760 | Powder pattern unindexed | | h6: $a$ = 509.2(8) $c$ = 1434(5) |
| $Li_2PtO_3$ | 29-820 | h6 | | |
| $Li_2SnO_3$ | (*16, 19*) | mC8 | XCR, NPR $C2/c$ | |
| | 31-761 | | $R$ = 10.5% for $n$ = 1462 | |
| | (*20*) | h6 | High-temp. form | |
| $Li_2PbO_3$ | 23-360 | o 24 | $hkl$ all even | h6: $a$ = 548.3(1) |
| | | | $b/a$ = 1.732 | $c$ = 1509.5(3) |
| $Na_2CeO_3$ | (*21*) | cF4/3 | | |
| $Na_2TbO_3$ | 21-1162 | o 12 | $b/a$ = 1.731 | h6: $a$ = 578.9(5) |
| | | | | $c$ = 1660(4) |
| $Na_2ZrO_3$ | 8-242 | mC24 | $hkl$ all even | mC4: $a$ = 547.7, $b$ = 971.5 |
| | | | | $c$ = 574.5, $\beta$ = 110.9° |
| | 21-1179 | h48 | Other supercell | |
| $Na_2HfO_3$ | (*2*) | o 12 | $b/a$ = 1.730 | h6: $a$ = 558.3(4) |
| | | | | $c$ = 1640(2) |
| $Na_2RuO_3$ | (*15*) | Pseudo-h6 | | |
| $Na_2PtO_3$ | 12-97 | o 24 | $hkl$ all even | h6: $a$ = 539.9(4) |
| | | | $b/a$ = 1.733 | $c$ = 1586(2) |
| | $\alpha$: 27-774 | mC8 | $hkl$ all odd or all even | h6: $a$ = 541.9(2) |
| | | | $\Delta\beta$ = 0.1°, $b/a$ = 1.734 | $c$ = 1590.4(7) |
| | $\beta$ (*15*): | oF16 | Other supercell | |
| $Na_2SnO_3$ | 30-1252 | tc (?) | Indexation in h6 includes | h6: $a$ = 552.8(3) |
| | | | 2 lines unindexed in tc | $c$ = 1639.3(14) |
| $Na_2PbO_3$ | (*2*) "*B*": 8-245 | cF4/3 | | |
| | "*A*": 8-251 | mC24 | $hkl$ all even | h6: $a$ = 568.3(3) |
| | | | | $c$ = 1641(1) |

[a] Unbracketed number = JCPDS reference.

[b] c, cubic; h, hexagonal; m, monoclinic; o, orthorhombic, tc = triclinic; C, F, I, usual Bravais lattice symbols; numerals, $Z$ value.

[c] XCR, X-ray single-crystal refinement; NPR, neutron profile refinement; $n$, number of independent reflections; $\Delta\beta = \beta$(m cell) $- \beta$(o cell).

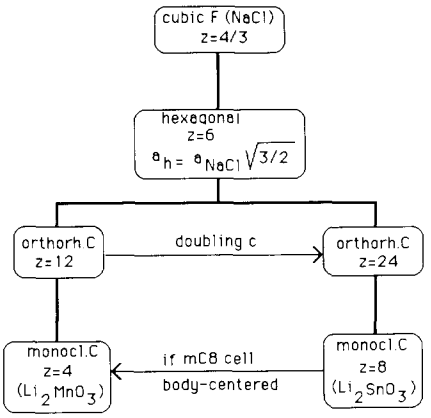


FIG. 5. Relationships between various cells for rocksalt-related $A_2BO_3$ compounds.

triclinic cell unrelated to rocksalt-type supercells) fit very well the smaller mC4 or h6 cell. The latter corresponds to the third stacking case predicted by Lang (*2*). Corrected parameters (obtained from least-square fitting of the literature or JCPDS data) are given in Table IV. The relationships between these various cells are given in Fig. 5.

## Conclusion

The single-crystal structure determination of $Li_2MnO_3$ has shown that the actual cell is a $Z = 4$ cell with $C2/m$ space group. The magnetic cell below $T_N$ is doubled along **c** and consists most probably of antiparallel layers of Mn spins along **c**. The powder used for this determination was slightly disordered. A survey of literature data shows that cationic disorder in rocksalt-type-related structures is commonplace and can provide an explanation for the variety of cell symmetries reported from X-ray powder data.

## Acknowledgment

The authors thank J. Pannetier (Institut Laue-Langevin) for his assistance in the neutron diffraction experiments and for helpful discussions.

## References

1. P. STROBEL, J. P. LEVY, AND J. C. JOUBERT, *J. Crystal Growth* **66,** 257 (1984).
2. G. LANG, *Z. Anorg. Allg. Chem.* **348,** 246 (1966).
3. M. JANSEN AND R. HOPPE, *Z. Anorg. Allg. Chem.* **397,** 279 (1973).
4. G. MEYER AND R. HOPPE, *Z. Anorg. Allg. Chem.* **424,** 257 (1976).
5. J. B. GOODENOUGH, *Phys. Rev.* **117,** 1442 (1960).
6. A. YOSHIMORI, *J. Phys. Soc. Japan* **14,** 807 (1959).
7. A. NØRLUND CHRISTENSEN AND G. OLLIVIER, *J. Solid State Chem.* **4,** 131 (1972).
8. D. E. COX, G. SHIRANE, R. J. BIRGENEAU, AND J. B. MCCHESNEY, *Phys. Rev.* **188,** 930 (1969).
9. R. D. SHANNON, *Acta Crystallogr. Sect. A* **32,** 751 (1976).
10. E. F. BERTAUT, *Acta Crystallogr. Sect. A* **24,** 217 (1968).
11. "Program AFFIST," Argonne Library (1980).
12. P. WOLFERS, A. M. S. Library, Institut Laue-Langevin, Grenoble (1976).
13. V. F. SEARS, Atomic Energy of Canada Report AECL-8490 (1984).
14. R. E. WATSON AND A. J. FREEMAN, *Acta Crystallogr.* **14,** 27 (1961).
15. J. HAUCK, *Acta Crystallogr. Sect. A* **36,** 228 (1980).
16. J. L. HODEAU, M. MAREZIO, A. SANTORO, AND R. S. ROTH, *J. Solid State Chem.* **45,** 170 (1982).
17. J. F. DORRIAN AND R. E. NEWNHAM, *Mater. Res. Bull.* **4,** 179 (1969).
18. J. M. REAU, M. POUCHARD, AND P. HAGENMULLER, *Bull. Soc. Chim. Fr.*, 4294 (1967).
19. G. KREUZBURG, F. STEWNER, AND R. HOPPE, *Z. Anorg. Allg. Chem.* **379,** 242 (1970).
20. M. TRÖMEL AND J. HAUCK, *Z. Anorg. Allg. Chem.* **373,** 8 (1970).
21. R. W. G. WYKOFF, "Crystal Structures," 2nd ed., Vol. 2, p. 532, Interscience, New York (1967).
22. W. URLAND AND R. HOPPE, *Z. Anorg. Allg. Chem.* **392,** 23 (1972).